

Tracking Control of Differential-Drive Wheeled Mobile Robots Using a Backstepping-Like Feedback Linearization

Dongkyoung Chwa

Abstract—This paper proposes a tracking control method for differential-drive wheeled mobile robots with nonholonomic constraints by using a backstepping-like feedback linearization. Unlike previous backstepping controllers for wheeled mobile robots, a backstepping-like feedback control structure is proposed in the form of a cascaded kinematic and dynamic linearization to have a simpler and modular control structure. First, the pseudo commands for the forward linear velocity and the heading direction angle are designed based on kinematics. Then, the actual torque control inputs are designed to make the actual forward linear velocity and heading direction angle follow their corresponding pseudo commands. A stability analysis shows that the tracking errors of the posture (the position and heading direction angle) are globally ultimately bounded and its ultimate bound can be adjusted by the proper choice of control parameters. In addition, numerical simulations for various reference trajectories (e.g., a straight line, a circle, a sinusoidal curve, a spinning trajectory with no forward velocity and a nonzero rotational velocity, a cross-shaped trajectory changing the forward and backward directions, etc.) show the validity of the proposed scheme.

Index Terms—Backstepping-like feedback linearization, nonholonomic constraints, tracking control, wheeled mobile robots.

I. INTRODUCTION

DIFFERENTIAL-drive wheeled mobile robots have restricted motion due to the nonholonomic constraints (where wheels are assumed to roll without slipping). They are also underactuated systems in which the number of control inputs is less than the number of states to be controlled; that is, there are two control inputs (the torques of two wheels) and three states to be controlled (the two position variables in a 2-D plane and a heading direction angle). Accordingly, many areas on mobile robots have drawn much attention [1]–[7]. In particular, as a linearized mobile robot model becomes deficient in controllability and the linear control method cannot be employed [8], many nonlinear control laws for mobile robots [9]–[20] have been proposed. Several other kinds of control laws have been studied, such as fuzzy logic control [21], role switching (or task switching) [22], separate designs of

Manuscript received November 14, 2003; revised January 30, 2007 and October 1, 2008. Date of publication August 9, 2010; date of current version October 15, 2010. This work was supported by the Korean government (Ministry of Education, Science and Technology) under Korea Science and Engineering Foundation Grant 2009-0069742. This paper was recommended by Associate Editor W. A. Gruver.

The author is with the Department of Electrical and Computer Engineering, Ajou University, Suwon 443-749, Korea (e-mail: dkchwa@ajou.ac.kr).

Digital Object Identifier 10.1109/TSMCA.2010.2052605

kinematic control inputs (forward and angular velocities), and dynamic control inputs (torques) [23], [24].

A global tracking control was achieved with respect to arbitrary initial tracking errors in [9] and [10], but the desired linear and angular velocities were constrained. These constraints were eliminated in [11], which, however, requires the adjustment of a control parameter that depends on the reference trajectories, and a persistently excited control input. A combined trajectory tracking and path following control has been proposed in [12]. Even though rigorous analyses of the stability and performance were performed, the nonlinear control methods for mobile robots are usually quite complicated. In particular, in the case of backstepping methods [9], [10], their applicability has a limitation in that the computation effort is too large to be implemented in real time. Thus, from the viewpoint of a practical application, it is desirable to have a modular structure so that various dynamic controllers (PID controllers, feedback linearization controllers, etc.) can be employed. Whereas the ideas encompassing the separate design of pseudo commands for forward linear and angular velocities based on kinematics and the low-level control based on dynamics were studied earlier in [23] and [24], the overall stability analysis of the position and heading direction angle errors is achieved without considering the dynamic tracking errors (i.e., the difference between the commanded forward linear and angular velocities and the actual ones). Although the backstepping methods in [9] and [10] had rigorous stability analyses performed, they suffer from the aforementioned problem.

To this end, this paper proposes a backstepping-like feedback control structure in the form of a cascaded kinematic and dynamic linearization. The proposed method is motivated by the fact that trajectory tracking can be achieved as long as zero position tracking errors are maintained and the heading direction angle is properly adjusted in either the forward or backward direction (refer to Fig. 1). With this in mind, the pseudo commands for the forward linear velocity and the heading direction angle are designed when performing the kinematic linearization. Then, the actual torque inputs are designed when performing the dynamic linearization so that the actual forward linear velocity and heading direction angle follow the pseudo commands (refer to Fig. 2). Thus, the proposed method is advantageous in that it has a much simpler and modular control structure, as compared to the regular backstepping method, and also in that the overall stability analysis considering the kinematic and dynamic linearizations is performed. Furthermore, the proposed method can change the actual moving direction of

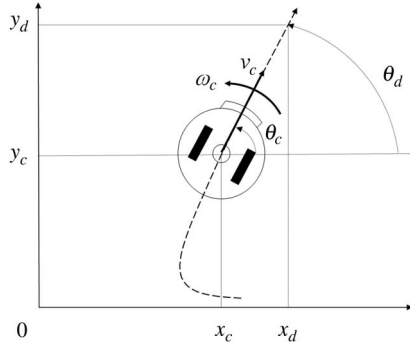


Fig. 1. Coordinates of the mobile robot and (dashed) the reference trajectory.

robots that can move either forward or backward by properly determining the pseudo heading direction angle, unlike in [13] and [14]. Whereas the sign of the forward linear velocity was just determined by the initial posture of the actual robot in [13] and thus cannot be employed in the system moving only in the forward direction, the kinematic time-invariant control method found in [14] can only maintain the motion in the forward direction. Uncertainty compensation is also an important issue. Uncertainties in the motion of actual mobile robots degrade the control performance, and accordingly, these uncertainties need to be compensated for by using adaptive control [15], [16] or sliding mode control [17]. Robust tracking control issues are briefly discussed in this paper by slightly modifying the proposed tracking control method. Finally, a stability analysis and simulations are performed to evaluate the tracking performance of the proposed method for reference trajectories such as a straight line, a circle, a sinusoidal curve, a spinning trajectory with no forward linear velocity and a nonzero rotational velocity, and a cross-shaped trajectory using the changing of the forward and backward directions.

II. DYNAMICS AND KINEMATICS OF WHEELED MOBILE ROBOTS

In this section, the dynamics and kinematics of wheeled mobile robots are briefly presented considering the nonholonomic constraints as found in [18]–[20]. Under nonholonomic constraints, Euler–Lagrange formulation [20] gives the dynamic equations given by

$$M(q)\ddot{q} + V(q, \dot{q})\dot{q} + G(q) = B(q)\tau + A^T(q)\lambda \quad (1)$$

where $q \in R^n$ is the generalized coordinates, $\tau \in R^r$ is a torque control input vector, $\lambda \in R^m$ is a constraint force vector, $M(q) \in R^{n \times n}$ is a symmetric and positive definite inertia matrix, $V(q, \dot{q}) \in R^{n \times n}$ is a centripetal and Coriolis matrix, $G(q) \in R^n$ is a gravitation vector, $B(q) \in R^{n \times r}$ is an input transformation matrix, $A(q) \in R^{m \times n}$ is a matrix related with nonholonomic constraints, and $r = n - m$ is assumed.

The nonholonomic kinematic constraints $A(q)\dot{q} = 0$ give $A(q)S(q) = 0$, where $S(q) \in R^{n \times (n-m)} = R^{n \times r}$ is composed of linearly independent vectors in the null space of $A(q)$. Thus, we can have $\dot{q} = S(q)z$, where an internal state variable z is an

$(n - m)$ -dimensional vector. Therefore, the dynamic equations of wheeled mobile robots can be given by

$$H(q)\dot{z} + F(q, z) = \tau \quad (2)$$

where $q^T = [x_c \ y_c \ \theta_c]$ and $z^T = [v_c \ \omega_c]$. As shown in Fig. 1, x_c and y_c are position variables, θ_c is a heading direction angle, v_c is a forward linear velocity, ω_c is an angular velocity of the mobile robot, $\tau = [\tau_l \ \tau_r]^T$ is a torque vector for left and right wheels, $H(q) = [S^T(q)B(q)]^{-1}S^T(q)M(q)S(q)$, $F(q, z) = [S^T(q)B(q)]^{-1}S^T(q)[\{M(q)S(q) + V(q, \dot{q})S(q)\}z + G(q)]$, and $S(q)$ is a null space of $A(q)$ given by

$$S^T(q) = \begin{pmatrix} \cos \theta_c & \sin \theta_c & 0 \\ 0 & 0 & 1 \end{pmatrix}.$$

The details can be referred to in [25].

Fig. 1 shows the coordinates of the mobile robot and the reference trajectory (which will be described in (3) later), where the reference trajectory moves along a curved line and then a straight line in the *forward* direction and the mobile robot tracks the reference trajectory in the same forward direction. The equation $A(q)\dot{q} = 0$, which is a nonholonomic constraint on the rolling motion of the robot wheel without slipping, can be expressed as $\dot{x}_c \sin \theta_c - \dot{y}_c \cos \theta_c = 0$. Also, a kinematic equation in Cartesian coordinates given by $\dot{q} = S(q)z$ can be expressed as

$$\begin{pmatrix} \dot{x}_c \\ \dot{y}_c \\ \dot{\theta}_c \end{pmatrix} = \begin{pmatrix} v_c \cos \theta_c \\ v_c \sin \theta_c \\ \omega_c \end{pmatrix}. \quad (3)$$

III. TRACKING CONTROL USING BACKSTEPPING-LIKE FEEDBACK LINEARIZATION

Based on the expression in (3), we consider a reference trajectory given by

$$\begin{cases} \dot{x}_d = v_d \cos(\theta_d) \\ \dot{y}_d = v_d \sin(\theta_d) \\ \dot{\theta}_d = \omega_d \end{cases} \quad (4)$$

where x_d and y_d are position variables of the reference, θ_d is a heading direction angle of the reference, v_d is a reference forward linear velocity, and ω_d is a reference angular velocity. It should be noted here that, since the filtered reference trajectory can be used to have derivatives, there is no loss of generality in assuming that the time derivatives of the position and heading direction angle of the reference trajectory are bounded.

The control objective is to make the mobile robots follow the desired trajectory in such a way that the position and heading direction angle tracking errors

$$x_e = x_c - x_d \quad y_e = y_c - y_d \quad \theta_e = \theta_c - \theta_d \quad (5)$$

reduce to zero by using the control input vector τ with two elements. For the tracking control of this underactuated system, we propose a control method in such a way that the position tracking errors are maintained at zero and the heading direction is determined in either the forward or backward direction.

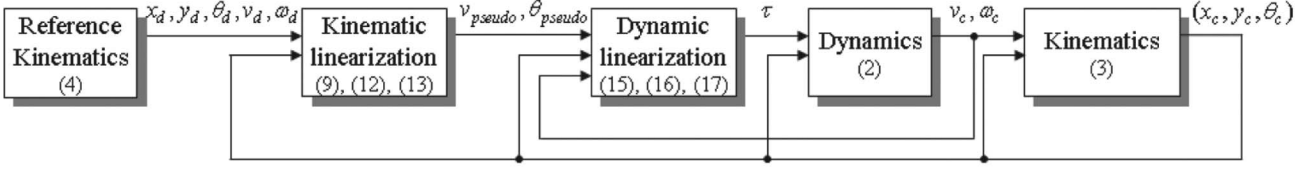


Fig. 2. Tracking control of wheeled mobile robots using backstepping-like feedback linearization.

In the proposed method shown in Fig. 2, the pseudo commands for the forward linear velocity v_{pseudo} and the heading direction angle θ_{pseudo} are first designed, and then, the actual torque input τ is designed to make the actual forward linear velocity v_c and heading direction angle θ_c follow the pseudo commands.

First, we introduce the variables

$$X := \dot{x}_d - k_p \tanh(x_e/k_p) \quad Y := \dot{y}_d - k_p \tanh(y_e/k_p) \quad (6)$$

for $k_p > 0$ such that the first two rows in (4) become

$$\begin{cases} \dot{x}_e + k_p \tanh(x_e/k_p) = v_c \cos(\theta_c) - X \\ \dot{y}_e + k_p \tanh(y_e/k_p) = v_c \sin(\theta_c) - Y \end{cases} \quad (7)$$

It should be noted that the introduction of X and Y in (6) is advantageous in the derivation of Theorem 1, given later, in that X and Y are bounded and also the expression of \dot{X} in (23a) and \dot{Y} in (23b) can be simplified. Then, for the position tracking (i.e., the convergence of x_e and y_e to zero), we can see from (7) that v_c and θ_c are required to make $\tilde{x}_e := v_c \cos(\theta_c) - X$ and $\tilde{y}_e := v_c \sin(\theta_c) - Y$ converge to zero, which corresponds to making

$$\cos(\theta_c)\tilde{x}_e + \sin(\theta_c)\tilde{y}_e = v_c - \cos(\theta_c)X - \sin(\theta_c)Y \quad (8a)$$

$$-\sin(\theta_c)\tilde{x}_e + \cos(\theta_c)\tilde{y}_e = \sin(\theta_c)X - \cos(\theta_c)Y \quad (8b)$$

converge to zero. Thus, based on (8a), the pseudo forward linear velocity v_{pseudo} for position tracking can be selected as

$$v_{\text{pseudo}} = \cos(\theta_c)X + \sin(\theta_c)Y. \quad (9)$$

Next, the pseudo heading direction angle θ_{pseudo} needs to be determined, considering both the position tracking and the yaw angle tracking. Using $\theta^* := \text{atan2}(Y, X)$, where $\text{atan2}(y, x)$ is a four-quadrant inverse tangent with the values in the interval of $[-\pi, \pi]$, (9) becomes

$$v_{\text{pseudo}} = \cos(\theta_c - \theta^*)\sqrt{X^2 + Y^2} \quad (10)$$

which is positive for $|\theta_c - \theta^*| < (\pi/2)$ and negative for $|\pi - (\theta_c - \theta^*)| < (\pi/2)$. Since the reference velocity v_d is positive (respectively, negative) in the case of forward (respectively, backward) motion, the pseudo heading direction angle should be selected in such a way that v_c and v_d have the same sign. That is, when v_d is positive (respectively, negative), v_c should also be positive (respectively, negative) so that $\theta_c - \theta^*$ satisfies $|\theta_c - \theta^*| < (\pi/2)$ [respectively, $|\pi - (\theta_c - \theta^*)| < (\pi/2)$], as can be seen from (10). From (8b), we should have

$$\sin(\theta_c)X - \cos(\theta_c)Y = \sin(\theta_c - \theta^*)\sqrt{X^2 + Y^2} = 0. \quad (11)$$

That is, θ_c should be θ^* or $\theta^* + \pi$. Thus, in the case of a positive v_d , we should have

$$\theta_{\text{pseudo}} = \theta^* \quad (12)$$

since v_{pseudo} becomes positive when $\theta_c = \theta_{\text{pseudo}}$ is satisfied. Similarly, in the case of a negative v_d , we should have

$$\theta_{\text{pseudo}} = \theta^* + \pi \quad (13)$$

to have negative v_{pseudo} . Here, we can see that both (12) and (13) satisfy

$$X \sin(\theta_{\text{pseudo}}) = Y \cos(\theta_{\text{pseudo}}) \quad (14)$$

i.e., (8b) becomes zero when $\theta = \theta_{\text{pseudo}}$. When $v_d = 0$, θ_{pseudo} in either (13) or (14) can be chosen, depending on the situation of whether we want the wheeled mobile robot to move in either the forward or backward direction. This situation is set as Scenario 5 in Section IV (simulation results), in which case, as well, the tracking performance can be satisfied, as will be shown in Fig. 7.

Remark 1: The pseudo command θ_{pseudo} in (12) or (13) implies that the heading direction angle is always driven to the trajectory, as in the pursuit guidance law [26]. In general, when only the position is controlled, the mobile robot may turn around and follow the reference trajectory backward. This situation, however, does not happen in the proposed method where the pseudo heading direction angle is generated as in (12) or (13) according to the sign of v_d .

Remark 2: The proposed method shown in Figs. 1 and 2 is developed by modifying the two-step linearization method for vertical take-off and landing (VTOL) aircraft in [27]. The significant difference between them is that the proposed method can be employed for the wheeled mobile robot which can move in both the forward and backward directions, whereas the two-step linearization method studied for VTOL aircraft has a restrictive posture due to the limited range of roll angle.

In the system dynamics of (2), $H(q)$ and $F(q, z)$ are assumed to be known. It remains to design the control input τ in such a way that v_c and θ_c follow v_{pseudo} and θ_{pseudo} . Instead of the backstepping or recursive design which involves the time derivative of θ_{pseudo} and results in the complicated control structure, a high-gain design feedback is employed to dominate \dot{v}_{pseudo} and $\dot{\theta}_{\text{pseudo}}$, as seen in [28].

Using the computed-torque method, a torque control input τ can be chosen from (2) as

$$\tau = F(q, z) + H(q)u \quad (15)$$

to have $\dot{z} = u$, and the corresponding control input u is proposed as

$$u = -Az + z_c \quad (16)$$

where $A = \text{diag}(k_v, a) > 0$ and

$$z_c = [k_v v_{\text{pseudo}}, b \sin(\theta_c - \theta_{\text{pseudo}})]^T \quad (17)$$

to have

$$\begin{aligned} \dot{v}_c &= -k_v v_c + k_v v_{\text{pseudo}} \\ \dot{\theta}_c &= \omega_c \\ \dot{\omega}_c &= -a\omega_c + b \sin(\theta_c - \theta_{\text{pseudo}}) \end{aligned} \quad (18)$$

where $a = 2\zeta k_\omega$ and $b = k_\omega^2$ for a positive constant $0 < \zeta \leq 1$ and k_v and k_ω are the high gains of the v_c and θ_c systems implying the asymptotic convergence of v_c and θ_c to v_{pseudo} and θ_{pseudo} .

Remark 3: Suppose that $z_c = [k_v v_{\text{pseudo}}, b(\theta_c - \theta_{\text{pseudo}})]^T$ is chosen instead of (17). Then, there can be a numerical discontinuity in the yaw angle near 0 and 2π ; e.g., ε and $2\pi - \varepsilon$ are physically almost the same for a very small ε angle, but the numerical difference is almost 2π . Thus, a sine function is introduced in (17) so that the second and third rows of (18) result in $\ddot{\theta}_c + a\dot{\theta}_c + b \sin(\theta_c - \theta_{\text{pseudo}}) = 0$, which is analyzed in the proof of the following theorem.

The stability and performance of the aforementioned kinematic and dynamic control system can be summarized as the following theorem.

Theorem 1: Control inputs $\tau = [\tau_l \ \tau_r]^T$ in (15) using v_{pseudo} in (9) and θ_{pseudo} in (12) [respectively, (13)] in the case of a positive (respectively, a negative) v_d guarantee the global ultimate boundedness of the tracking errors in (5) and the yaw angle tracking error for control parameters k_p and k_v satisfying $k_p > 0$ and $k_v > 1$. The ultimate bounds of the tracking errors are dependent on E_θ ($:= \theta_c - \theta_{\text{pseudo}}$), \dot{x}_d , \ddot{x}_d , \dot{y}_d , \ddot{y}_d , and ω_c and can be made smaller with the proper choice of k_p , k_ω , and k_v . The boundedness of ω_c is guaranteed, and the magnitude of E_θ is dependent on $|a\dot{\theta}_{\text{pseudo}} + \ddot{\theta}_{\text{pseudo}}|$, which can be reduced to zero in the case that the reference trajectory is a straight line. Here, $\dot{\theta}_{\text{pseudo}}$ and $\ddot{\theta}_{\text{pseudo}}$ are the first- and second-order time derivatives, respectively.

Proof: The first and second rows of (3) become

$$\begin{aligned} \dot{x}_c &= E_v \cos(\theta_c) + v_{\text{pseudo}} \cos(\theta_c) \\ &= E_v \cos(\theta_c) + \cos^2(\theta_c)X + \sin(\theta_c) \cos(\theta_c)Y \\ &= E_v \cos(\theta_c) + \cos^2(\theta_c)X + \sin(\theta_c) \\ &\quad \times [\cos(\theta_{\text{pseudo}})Y + \{\cos(\theta_c) - \cos(\theta_{\text{pseudo}})\}Y] \\ &= E_v \cos(\theta_c) + \cos^2(\theta_c)X + \sin(\theta_c) \\ &\quad \times [\sin(\theta_c)X + \{\sin(\theta_{\text{pseudo}}) - \sin(\theta_c)\}X \\ &\quad + \{\cos(\theta_c) - \cos(\theta_{\text{pseudo}})\}Y] \\ &= E_v \cos(\theta_c) + X + \sin(\theta_c) \\ &\quad \times [\{\sin(\theta_{\text{pseudo}}) - \sin(\theta_c)\}X \end{aligned}$$

$$\begin{aligned} &\quad + \{\cos(\theta_c) - \cos(\theta_{\text{pseudo}})\}Y] \\ &= X + E_v \cos(\theta_c) + \sin(\theta_c) \\ &\quad \times T(E_\theta, \theta_c, \theta_{\text{pseudo}}, X, Y) \end{aligned} \quad (19a)$$

$$\begin{aligned} \dot{y}_c &= E_v \sin(\theta_c) + v_{\text{pseudo}} \sin(\theta_c) \\ &= E_v \sin(\theta_c) + \sin^2(\theta_c)Y + \cos(\theta_c) \sin(\theta_c)X \\ &= E_v \sin(\theta_c) + \sin^2(\theta_c)Y + \cos(\theta_c) \\ &\quad \times [\sin(\theta_{\text{pseudo}})X + \{\sin(\theta_c) - \sin(\theta_{\text{pseudo}})\}X] \\ &= E_v \sin(\theta_c) + \sin^2(\theta_c)Y + \cos(\theta_c) \\ &\quad \times [\cos(\theta_c)Y + \{\cos(\theta_{\text{pseudo}}) - \cos(\theta_c)\}Y \\ &\quad + \{\sin(\theta_c) - \sin(\theta_{\text{pseudo}})\}X] \\ &= E_v \sin(\theta_c) + Y + \cos(\theta_c) \\ &\quad \times [\{\cos(\theta_{\text{pseudo}}) - \cos(\theta_c)\}Y \\ &\quad + \{\sin(\theta_c) - \sin(\theta_{\text{pseudo}})\}X] \\ &= Y + E_v \sin(\theta_c) - \cos(\theta_c) \\ &\quad \times T(E_\theta, \theta_c, \theta_{\text{pseudo}}, X, Y) \end{aligned} \quad (19b)$$

where the second and fourth equalities follow from (9) and (14), respectively, $E_v = v_c - v_{\text{pseudo}}$, and $T(E_\theta, \theta_c, \theta_{\text{pseudo}}, X, Y)$ satisfies

$$\begin{aligned} T(E_\theta, \theta_c, \theta_{\text{pseudo}}, X, Y) &= -\{\sin(\theta_c) - \sin(\theta_{\text{pseudo}})\}X \\ &\quad + \{\cos(\theta_c) - \cos(\theta_{\text{pseudo}})\}Y \\ &= -2 \sin\left(\frac{E_\theta}{2}\right) \cdot \left\{ \cos\left(\frac{\theta_c + \theta_{\text{pseudo}}}{2}\right)X \right. \\ &\quad \left. + \sin\left(\frac{\theta_c + \theta_{\text{pseudo}}}{2}\right)Y \right\}. \end{aligned}$$

It should be noted that $T(E_\theta, \theta_c, \theta_{\text{pseudo}}, X, Y)$ is bounded as X and Y are bounded and therefore decreases to zero as E_θ decreases to zero. Thus, (19a) and (19b) become

$$\begin{pmatrix} \dot{x}_e + k_p \tanh(x_e/k_p) \\ \dot{y}_e + k_p \tanh(y_e/k_p) \end{pmatrix} = \begin{pmatrix} \cos(\theta_c) & \sin(\theta_c) \\ \sin(\theta_c) & -\cos(\theta_c) \end{pmatrix} \times \begin{pmatrix} E_v \\ T(E_\theta, \theta_c, \theta_{\text{pseudo}}, X, Y) \end{pmatrix}. \quad (20)$$

Also, using (18), the time derivatives of E_v and ξ_1 ($:= E_\theta$) become

$$\begin{aligned} \dot{E}_v &= -k_v E_v - \dot{v}_{\text{pseudo}} \\ \dot{\xi}_1 &= \xi_2 \\ \dot{\xi}_2 &= -a\xi_2 - b \sin(\xi_1) - (a\dot{\theta}_{\text{pseudo}} + \ddot{\theta}_{\text{pseudo}}). \end{aligned} \quad (21)$$

Now, we choose the Lyapunov candidate as $V = V_1 + V_2$, where $V_1 = k_p \cdot [\ln\{\cosh(x_e/k_p)\} + \ln\{\cosh(y_e/k_p)\}]$, $V_2 = (1/2)\zeta_2^T \zeta_2$, and $\zeta_2 = E_v$, and introduce $\zeta_1 := [\zeta_{1x} \ \zeta_{1y}]^T =$

$[\tanh(x_e/k_p) \quad \tanh(y_e/k_p)]^T$. Consequentially, (20) and (21) give

$$\begin{aligned} \dot{V} &= -k_p\zeta_1^T\zeta_1 - k_v\zeta_2^2 + \zeta_1^T \begin{pmatrix} \cos(\theta_c) & \sin(\theta_c) \\ \sin(\theta_c) & -\cos(\theta_c) \end{pmatrix} \\ &\quad \cdot \begin{pmatrix} \zeta_2 \\ T(\xi_1, \theta_c, \theta_{\text{pseudo}}, X, Y) \end{pmatrix} + (-\dot{v}_{\text{pseudo}})\zeta_2 \\ &= -k_p\zeta_1^T\zeta_1 - k_v\zeta_2^2 + \zeta_1^T \begin{pmatrix} \cos(\theta_c) & \sin(\theta_c) \\ \sin(\theta_c) & -\cos(\theta_c) \end{pmatrix} \\ &\quad \cdot \begin{pmatrix} \zeta_2 \\ T(\xi_1, \theta_c, \theta_{\text{pseudo}}, X, Y) \end{pmatrix} \\ &\quad - \zeta_2 \left\{ -\sin(\theta_c)\omega_c X + \cos(\theta_c)\dot{X} \right. \\ &\quad \left. + \cos(\theta_c)\omega_c Y + \sin(\theta_c)\dot{Y} \right\} \\ &= -k_p\zeta_1^T\zeta_1 - k_v\zeta_2^2 \\ &\quad - \zeta_2 \left\{ -\sin(\theta_c)\omega_c X + \cos(\theta_c)\omega_c Y \right. \\ &\quad \left. + \cos(\theta_c)(\dot{X} - \zeta_{1x}) + \sin(\theta_c)(\dot{Y} - \zeta_{1y}) \right\} \\ &\quad + T(\xi_1, \theta_c, \theta_{\text{pseudo}}, X, Y) \cdot (\sin(\theta_c)\zeta_{1x} - \cos(\theta_c)\zeta_{1y}) \end{aligned} \quad (22)$$

where (9) is used in deriving the second equality. The time derivatives of (6) can be given by

$$\begin{aligned} \dot{X} &= \ddot{x}_d - \operatorname{sech}^2(x_e/k_p) \{ v_c \cos(\theta_c) - \dot{x}_d \} \\ &= \ddot{x}_d + \operatorname{sech}^2(x_e/k_p) \dot{x}_d - \operatorname{sech}^2(x_e/k_p) \\ &\quad \times \{ v_{\text{pseudo}} \cos(\theta_c) + \zeta_2 \cos(\theta_c) \} \\ &= \ddot{x}_d + \operatorname{sech}^2(x_e/k_p) \dot{x}_d - \operatorname{sech}^2(x_e/k_p) \\ &\quad \times \{ \cos^2(\theta_c)X + \cos(\theta_c)\sin(\theta_c)Y + \zeta_2 \cos(\theta_c) \} \\ &= \ddot{x}_d + \operatorname{sech}^2(x_e/k_p) \dot{x}_d - \operatorname{sech}^2(x_e/k_p)X - \operatorname{sech}^2(x_e/k_p) \\ &\quad \times \{ -\sin^2(\theta_c)X + \cos(\theta_c)\sin(\theta_c)Y + \zeta_2 \cos(\theta_c) \} \\ &= \ddot{x}_d + k_p \operatorname{sech}^2(x_e/k_p) \tanh(x_e/k_p) - \operatorname{sech}^2(x_e/k_p) \\ &\quad \cdot \{ -\sin^2(\theta_c)X + \cos(\theta_c)\sin(\theta_c)Y + \zeta_2 \cos(\theta_c) \} \\ &= X_c + X_x \zeta_{1x} + X_y \zeta_{1y} - \operatorname{sech}^2(x_e/k_p) \zeta_2 \cos(\theta_c) \end{aligned} \quad (23a)$$

$$\begin{aligned} \dot{Y} &= \ddot{y}_d - \operatorname{sech}^2(y_e/k_p) \{ v_c \sin(\theta_c) - \dot{y}_d \} \\ &= \ddot{y}_d + \operatorname{sech}^2(y_e/k_p) \dot{y}_d - \operatorname{sech}^2(y_e/k_p) \\ &\quad \cdot \{ \cos(\theta_c)\sin(\theta_c)X + \sin^2(\theta_c)Y + \zeta_2 \sin(\theta_c) \} \\ &= \ddot{y}_d + \operatorname{sech}^2(y_e/k_p) \dot{y}_d - \operatorname{sech}^2(y_e/k_p)Y - \operatorname{sech}^2(y_e/k_p) \\ &\quad \times \{ \cos(\theta_c)\sin(\theta_c)X - \cos^2(\theta_c)Y + \zeta_2 \sin(\theta_c) \} \\ &= \ddot{y}_d + k_p \operatorname{sech}^2(y_e/k_p) \tanh(y_e/k_p) - \operatorname{sech}^2(y_e/k_p) \\ &\quad \cdot \{ \cos(\theta_c)\sin(\theta_c)X - \cos^2(\theta_c)Y + \zeta_2 \sin(\theta_c) \} \\ &= Y_c + Y_x \zeta_{1x} + Y_y \zeta_{1y} - \operatorname{sech}^2(y_e/k_p) \zeta_2 \sin(\theta_c) \end{aligned} \quad (23b)$$

where (9) is used in deriving the third equalities, and

$$\begin{aligned} X_c &= \ddot{x}_d + \operatorname{sech}^2(x_e/k_p) \sin^2(\theta_c) \dot{x}_d \\ &\quad - \operatorname{sech}^2(x_e/k_p) \cos(\theta_c) \sin(\theta_c) \dot{y}_d \\ X_x &= -k_p \operatorname{sech}^2(x_e/k_p) \sin^2(\theta_c) \\ X_y &= k_p \operatorname{sech}^2(x_e/k_p) \cos(\theta_c) \sin(\theta_c) \\ Y_c &= \ddot{y}_d - \operatorname{sech}^2(y_e/k_p) \cos(\theta_c) \sin(\theta_c) \dot{x}_d \\ &\quad + \operatorname{sech}^2(y_e/k_p) \cos^2(\theta_c) \dot{y}_d \\ Y_x &= k_p \operatorname{sech}^2(y_e/k_p) \cos(\theta_c) \sin(\theta_c) \\ Y_y &= -k_p \operatorname{sech}^2(y_e/k_p) \cos^2(\theta_c) \end{aligned}$$

are bounded. Thus, (22) can be further changed as

$$\begin{aligned} \dot{V} &= -k_p\zeta_1^T\zeta_1 - k_v\zeta_2^2 - \zeta_2 \left\{ -\sin(\theta_c)\omega_c X + \cos(\theta_c)\omega_c Y \right. \\ &\quad \left. - \cos(\theta_c)\zeta_{1x} - \sin(\theta_c)\zeta_{1y} \right\} \\ &\quad - \zeta_2 \cos(\theta_c) [X_c + X_x \zeta_{1x} + X_y \zeta_{1y}] \\ &\quad - \operatorname{sech}^2(x_e/k_p) \zeta_2 \cos(\theta_c) \\ &\quad - \zeta_2 \sin(\theta_c) [Y_c + Y_x \zeta_{1x} + Y_y \zeta_{1y}] \\ &\quad - \operatorname{sech}^2(y_e/k_p) \zeta_2 \sin(\theta_c) \\ &\quad + T(\xi_1, \theta_c, \theta_{\text{pseudo}}, X, Y) \cdot \{ \sin(\theta_c)\zeta_{1x} - \cos(\theta_c)\zeta_{1y} \} \\ &= -k_p\zeta_1^T\zeta_1 - k_v\zeta_2^2 - \zeta_2 \left\{ -\cos(\theta_c)\zeta_{1x} - \sin(\theta_c)\zeta_{1y} \right\} \\ &\quad - \zeta_2 \cos(\theta_c) [\omega_c X + X_c + X_x \zeta_{1x} + X_y \zeta_{1y}] \\ &\quad - \operatorname{sech}^2(x_e/k_p) \zeta_2 \cos(\theta_c) \\ &\quad - \zeta_2 \sin(\theta_c) [-\omega_c X + Y_c + Y_x \zeta_{1x} + Y_y \zeta_{1y}] \\ &\quad - \operatorname{sech}^2(y_e/k_p) \zeta_2 \sin(\theta_c) \\ &\quad + T(\xi_1, \theta_c, \theta_{\text{pseudo}}, X, Y) \{ \sin(\theta_c)\zeta_{1x} - \cos(\theta_c)\zeta_{1y} \} \\ &\leq -k_p\zeta_1^T\zeta_1 - (k_v - 1)\zeta_2^2 \\ &\quad + \left(\begin{matrix} \omega_c Y + X_c + (X_x - 1)\zeta_{1x} + X_y \zeta_{1y} \\ -\omega_c X + Y_c + Y_x \zeta_{1x} + (Y_y - 1)\zeta_{1y} \end{matrix} \right)^T \\ &\quad \cdot \begin{pmatrix} -\cos(\theta_c) \\ -\sin(\theta_c) \end{pmatrix} \zeta_2 + T(\xi_1, \theta_c, \theta_{\text{pseudo}}, X, Y) \\ &\quad \cdot \{ \sin(\theta_c)\zeta_{1x} - \cos(\theta_c)\zeta_{1y} \} \\ &= -k_p\zeta_1^T\zeta_1 - (k_v - 1)\zeta_2^2 \\ &\quad + \left(\begin{matrix} \omega_c \dot{y}_d - \omega_c k_p \zeta_{1y} + X_c + (X_x - 1)\zeta_{1x} + X_y \zeta_{1y} \\ -\omega_c \dot{x}_d + \omega_c k_p \zeta_{1x} + Y_c + Y_x \zeta_{1x} + (Y_y - 1)\zeta_{1y} \end{matrix} \right)^T \\ &\quad \cdot \begin{pmatrix} -\cos(\theta_c) \\ -\sin(\theta_c) \end{pmatrix} \zeta_2 + T(\xi_1, \theta_c, \theta_{\text{pseudo}}, X, Y) \\ &\quad \cdot \{ \sin(\theta_c)\zeta_{1x} - \cos(\theta_c)\zeta_{1y} \} \\ &= -k_p\zeta_1^T\zeta_1 - (k_v - 1)\zeta_2^2 \\ &\quad + \left(\begin{matrix} -\omega_c k_p \zeta_{1y} + (X_x - 1)\zeta_{1x} + X_y \zeta_{1y} \\ \omega_c k_p \zeta_{1x} + Y_x \zeta_{1x} + (Y_y - 1)\zeta_{1y} \end{matrix} \right)^T \\ &\quad \cdot \begin{pmatrix} -\cos(\theta_c) \\ -\sin(\theta_c) \end{pmatrix} \zeta_2 + \left(\begin{matrix} \omega_c \dot{y}_d + X_c \\ -\omega_c \dot{x}_d + Y_c \end{matrix} \right)^T \begin{pmatrix} -\cos(\theta_c) \\ -\sin(\theta_c) \end{pmatrix} \zeta_2 \\ &\quad + T(\xi_1, \theta_c, \theta_{\text{pseudo}}, X, Y) \{ \sin(\theta_c)\zeta_{1x} - \cos(\theta_c)\zeta_{1y} \} \\ &\leq -k_p\zeta_1^T\zeta_1 - (k_v - 1)\zeta_2^2 + 2(1 + |\omega_c|k_p + 1.5k_p) \cdot |\zeta_2| \\ &\quad + |(\omega_c \dot{y}_d + X_c) \cos(\theta_c) + (-\omega_c \dot{x}_d + Y_c) \sin(\theta_c)| \cdot |\zeta_2| \\ &\quad + T(\xi_1, \theta_c, \theta_{\text{pseudo}}, X, Y) \{ \sin(\theta_c)\zeta_{1x} - \cos(\theta_c)\zeta_{1y} \} \\ &\leq -k_p \{ (\zeta_{1x} - A_x)^2 + (\zeta_{1y} - A_y)^2 \} \\ &\quad - (k_v - 1)(\zeta_2 - B)^2 + C \end{aligned} \quad (24)$$

where

$$\begin{aligned} A_x &= T(\xi_1, \theta_c, \theta_{\text{pseudo}}, X, Y) \sin(\theta_c)/(2k_p) \\ A_y &= T(\xi_1, \theta_c, \theta_{\text{pseudo}}, X, Y) \cos(\theta_c)/(2k_p) \\ B &= 1/\{2(k_v - 1)\} \\ &\quad \cdot \{2(1 + |\omega_c|k_p + 1.5k_p) \\ &\quad + |(\omega_c \dot{y}_d + X_c) \cos(\theta_c) + (-\omega_c \dot{x}_d + Y_c) \sin(\theta_c)|\} \\ C &= k_p (A_x^2 + A_y^2) + (k_v - 1)B^2. \end{aligned} \quad (25)$$

In (24), $|\text{sech}^2(x_e)|$, $|\text{sech}^2(y_e)| \leq 1$ are used in deriving the first inequality, and $|X_x|$, $|Y_y| \leq k_p$, $|X_y|$, $|Y_x| \leq 0.5k_p$, and $|\zeta_{1x}|$, $|\zeta_{1y}| \leq 1$ are used in deriving the second inequality.

To see the boundedness of $T(\xi_1, \theta_c, \theta_{\text{pseudo}}, X, Y)$, $\dot{\omega}_c + a\omega_c = b \sin E_\theta$ is obtained from (18), and thus, ω_c is guaranteed to be bounded. Also, $\omega_c \dot{y}_d + X_c$ and $-\omega_c \dot{x}_d + Y_c$ are bounded, and k_p and k_v are chosen in such a way that $k_p > 0$ and $k_v > 1$. From (25), we can see that the ultimate bounds are determined by ξ_1 , \dot{x}_d , \dot{y}_d , \ddot{x}_d , \ddot{y}_d , and ω_c . From the aforementioned arguments, ζ_1 and ζ_2 are guaranteed to be ultimately bounded, and the ultimate bound is dependent on ξ_1 , \dot{x}_d , \dot{y}_d , \ddot{x}_d , and \ddot{y}_d and can be adjusted by the proper choice of k_p , k_ω , and k_v (note that a and b in (18) are functions of k_ω).

Whereas \dot{x}_d , \dot{y}_d , \ddot{x}_d , and \ddot{y}_d are determined by the velocity of the reference trajectory, ξ_1 (or E_θ) can be adjusted to reduce the ultimate bound. We further choose a Lyapunov candidate as $W = 0.5a^2\xi_1^2 + a\xi_1\xi_2 + \xi_2^2 + 2b\{1 - \cos(\xi_1)\}$ from (18), where $\xi_2 = \dot{\xi}_1$. We can suppose here that $-\pi < \xi_1 \leq \pi$ without loss of generality. Therefore, the time derivative of W becomes

$$\begin{aligned} \dot{W} &= a^2\xi_1\dot{\xi}_1 + (a\xi_1\xi_2 + a\xi_1\dot{\xi}_2) + 2\xi_2\dot{\xi}_2 + 2b \sin(\xi_1)\dot{\xi}_1 \\ &= \{a^2\xi_1 + a\xi_2 + 2b \sin(\xi_1)\} \cdot \dot{\xi}_1 + (a\xi_1 + 2\xi_2) \cdot \dot{\xi}_2 \\ &= \{a^2\xi_1 + a\xi_2 + 2b \sin(\xi_1)\} \cdot \xi_2 + (a\xi_1 + 2\xi_2) \\ &\quad \cdot \{-a\xi_2 - b \sin(\xi_1) - (a\dot{\theta}_{\text{pseudo}} + \ddot{\theta}_{\text{pseudo}})\} \\ &= -ab\xi_1 \sin(\xi_1) - a\xi_2^2 \\ &\quad - (a\xi_1 + 2\xi_2)(a\dot{\theta}_{\text{pseudo}} + \ddot{\theta}_{\text{pseudo}}). \end{aligned} \quad (26)$$

As $\xi_1 \sin(\xi_1) \geq 0$ from $-\pi < \xi_1 \leq \pi$, the ultimate bound of ξ_1 is dependent on $|a\dot{\theta}_{\text{pseudo}} + \ddot{\theta}_{\text{pseudo}}|$. If the reference trajectory is a straight line, then θ_{pseudo} becomes constant, and $a\dot{\theta}_{\text{pseudo}} + \ddot{\theta}_{\text{pseudo}}$ reduces to zero. The combination of (24) and (26) shows that the ultimate bound can be made sufficiently small, as can be seen in the simulation results in Section IV. (Q.E.D.)

Remark 4: In an actual situation, the dynamics in (2) contain the uncertainties, and accordingly, the assumption of an exactly known dynamics employed for the design of the dynamic control law (15) may not be valid. As a solution for this, we can make the following assumption that the disturbances exist in system dynamics and modify (15), as seen in [17]. Suppose that the bounded disturbances τ_d exist in the system dynamics (2) as

$$H(q)\dot{z} + F(q, z) + \tau_d = \tau \quad (27)$$

where $\tau_d = H(q)f$, $f = [f_1 \ f_2]^T$, $|f_i| \leq f_{mi}$, $i = 1, 2$. In this case, instead of (15), a robust torque control input τ can be designed as

$$\tau = F(q, z) + H(q)(u + \bar{u}) \quad (28)$$

to have $\dot{z} = u + \bar{u} - f$ where

$$\bar{u} = - \left(\begin{array}{l} D_v \text{sgn}(v_c - v_{\text{pseudo}}) \\ D_\omega \text{sgn} \left\{ a(\theta_c - \theta_{\text{pseudo}}) + 2(\omega_c - \dot{\theta}_{\text{pseudo}}) \right\} \end{array} \right) \quad (29)$$

is used to compensate for the influence of f and D_v and D_ω are positive constants satisfying $f_{m1} \leq D_v$ and $f_{m2} \leq D_\omega$. The stability analysis can be done in the same way as in the proof of Theorem 1 by slightly modifying (21) as

$$\begin{aligned} \dot{E}_v &= -k_v E_v - \dot{v}_{\text{pseudo}} - f_1 - D_v \text{sgn}(E_v) \\ \dot{\xi}_1 &= \xi_2 \\ \dot{\xi}_2 &= -a\xi_2 - b \sin(\xi_1) - (a\dot{\theta}_{\text{pseudo}} + \ddot{\theta}_{\text{pseudo}}) - f_2 \\ &\quad - D_\omega \text{sgn} \left\{ a(\theta_c - \theta_{\text{pseudo}}) + 2(\omega_c - \dot{\theta}_{\text{pseudo}}) \right\}. \end{aligned} \quad (30)$$

The signum term in (29) can be replaced by a saturation function to reduce the chattering phenomenon in practical application [29]. In fact, it can be analyzed that (15) has a robustness against τ_d , which is also demonstrated in the simulation results in the next section.

IV. SIMULATION RESULTS

In this section, the simulation results from the differential-drive wheeled mobile robot using the proposed method in Table I are presented. The actual and reference kinematics are given by (3) and (4); $\dot{z} = u - f$ is used instead of (27) for the dynamics, which is valid by applying the computed-torque control (15)–(27). The disturbances $[f_1, f_2]$ used here are chosen to be Gaussian random noises with mean $[0, 0]$ and variance $[0.5 \text{ m}^2/\text{s}^2, 0.5 \text{ rad}^2/\text{s}^2]$. The dynamic controller is given by (15)–(17), and the kinematic controller is given by (9), (12), (13), and (6). The design parameters of the control law in (6), (16), and (17) are chosen as $k_p = 10$, $k_v = 100$, $k_\omega = 30$, and $\zeta = 0.7$, which satisfy the condition in Theorem 1 given by $k_p > 0$ and $k_v > 1$. Considering the actual mobile robots, saturation should exist in the (forward linear and angular) velocities and accelerations, which correspond to the saturation of the torque inputs from $\dot{z} = u - f$. Thus, we included the constraints

$$v_{\max} = 15 \text{ m/s} \quad \omega_{\max} = 20 \text{ rad/s} \quad (31a)$$

$$\dot{v}_{\max} = 10 \text{ m/s}^2 \quad \dot{\omega}_{\max} = 20 \text{ rad/s}^2 \quad (31b)$$

in the simulations. It should be noted that, when the input saturation values of the actual mobile robots are different from (31), the velocities of the reference trajectories and the initial posture tracking errors given in Table I should be adjusted for satisfactory trajectory tracking, which is not within the scope of this paper.

TABLE I
INITIAL CONDITIONS ON THE VELOCITIES AND POSTURE OF THE REFERENCE AND THE MOBILE ROBOT
(v_d (m/s): FORWARD LINEAR VELOCITY, ω_d (rad/s): ANGULAR VELOCITY)

	Reference velocities		Reference initial posture	Robot initial posture
	v_d	ω_d	($[x_d(0), y_d(0), \theta_d(0)]$) (m, m, rad)	($[x_c(0), y_c(0), \theta_c(0)]$) (m, m, rad)
Scenario 1	5	0	[0.707, 0.707, $\pi/4$]	[-19.758, 18.839, -0.38]
Scenario 2	5	-0.1	[0.707, 0.707, $\pi/2$]	[-5.283, 5.038, -0.38]
Scenario 3	-5	0.8	[10.607, 10.607, - $\pi/4$]	[-5.283, 5.038, -0.38]
Scenario 4	1	$0.1\sin(0.04\pi t)$	[0, 0, $7/4\pi$]	[17, 4, π]
Scenario 5	0	0.5	[0, 0, 0]	[27.3, 2.38, -0.38]
Scenario 6	$\text{sgn}\{\sin(2\theta_d)\}$	0.1	[1, 1, 1]	[0, 0, 0]

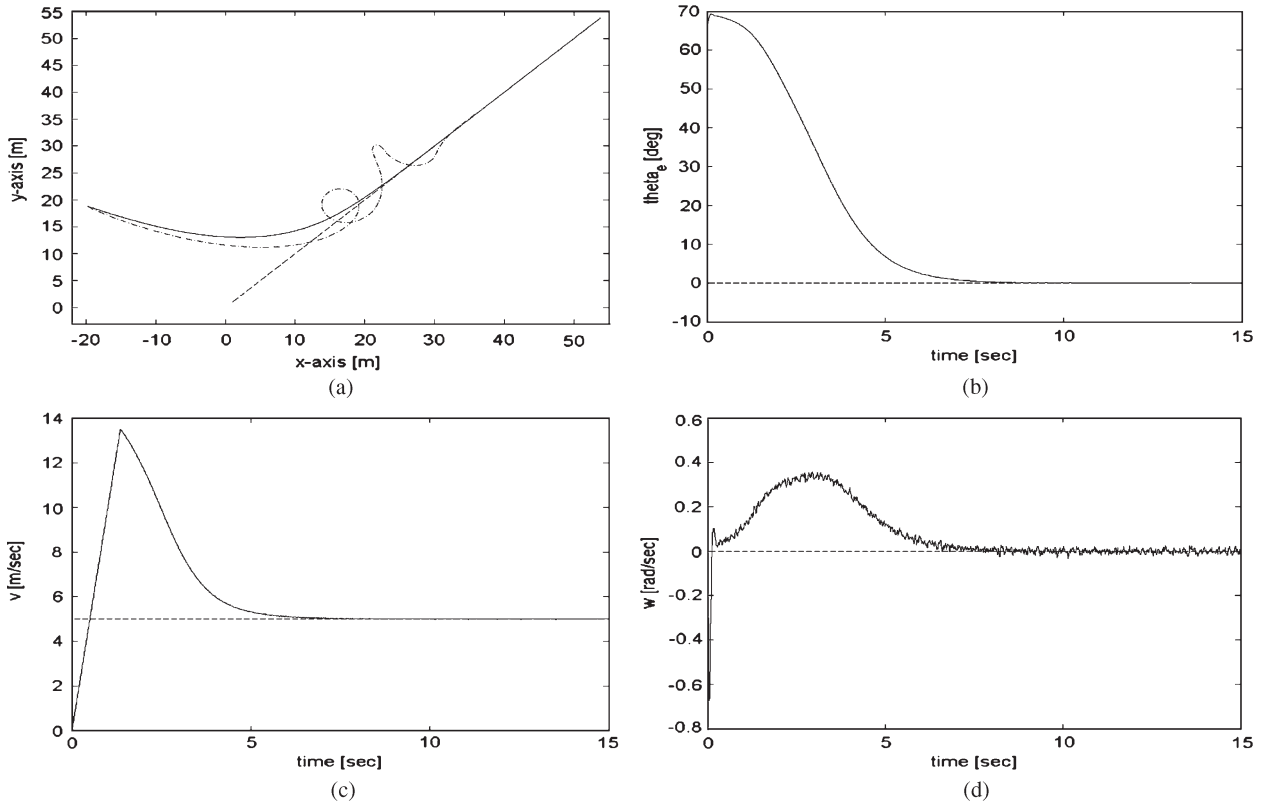


Fig. 3. Trajectory tracking performance of the proposed controller with input saturation (31) (Scenario 1). In (a), (c), and (d), (dashed) reference and (solid) proposed; in (a), (dashed-dotted) previous one [18]. (a) x - y plot. (b) Tracking error (θ_e). (c) Forward velocity v . (d) Angular velocity ω .

The reference trajectory is generated using the reference model in (4). The initial position and heading direction angle errors are assumed to exist as several scenarios, as in Table I, and the initial velocities are $(u(0), v(0), r(0)) = (0, 0, 0)$. The reference trajectories of each scenario are as follows: 1) a straight line; 2) a curve; 3) a circle in the backward direction; 4) a time-varying sinusoidal curve; 5) a spinning trajectory with no forward velocity and a nonzero rotational velocity ($v_d = 0, \omega_d \neq 0$); and 6) a cross-shaped trajectory with the changing of the forward and backward directions.

The tracking performance of the proposed method is compared with that of the previous method in [18]. The kinematic controller from [18] is chosen here as

$$\begin{aligned} v_{\text{pseudo}} &= v_r \cos(\bar{\theta}_e) + K_x \bar{x}_e \\ \omega_{\text{pseudo}} &= \omega_r + v_r \{K_y \bar{y}_e + K_\theta \sin(\theta_e)\} \end{aligned} \quad (32)$$

where $\bar{x}_e = \cos(\theta_c)x_e + \sin(\theta_c)y_e$, $\bar{y}_e = -\sin(\theta_c)x_e + \cos(\theta_c)y_e$, $K_x = 10$, $K_y = (\xi/v_d)^2$, $K_\theta = 2\zeta\sqrt{K_y}$, $\zeta = 0.707$, and $\xi = 2.4$. A simple dynamic controller is chosen as

$$u = -\bar{A}z + z_c \quad (33)$$

where $\bar{A} = \text{diag}(k_v, k_v) > 0$ and $z_c = [k_v v_{\text{pseudo}}, k_v \omega_{\text{pseudo}}]^T$ such that

$$\dot{v}_c = -k_v v_c + k_v v_{\text{pseudo}} \quad \dot{\omega}_c = -k_v \omega_c + k_v \omega_{\text{pseudo}}. \quad (34)$$

Figs. 3–8 show the tracking performance of the proposed method for Scenarios 1–6, respectively. As the reference forward velocity is negative in Scenarios 3 and 6 and also zero

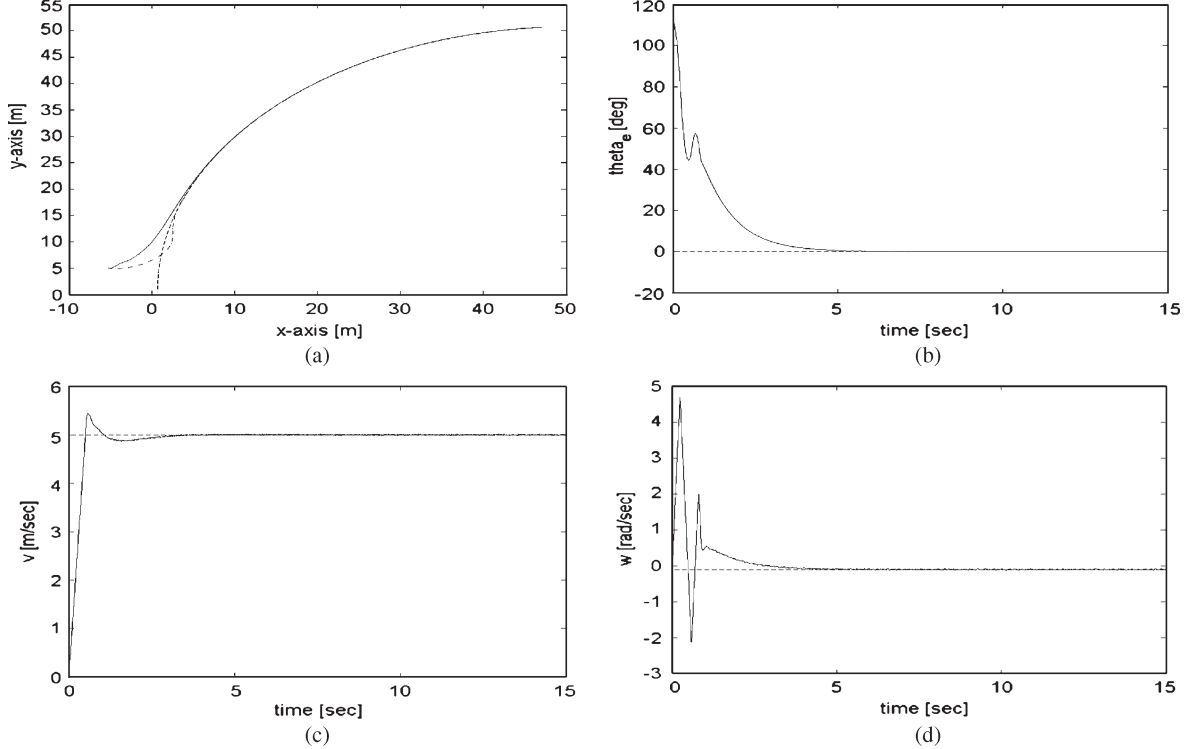


Fig. 4. Trajectory tracking performance of the proposed controller with input saturation (31) (Scenario 2). In (a), (c), and (d), (dashed) reference and (solid) proposed; in (a), (dashed-dotted) previous one [18]. (a) \$x\$-\$y\$ plot. (b) Tracking error (\$\theta_e\$). (c) Forward velocity \$v\$. (d) Angular velocity \$\omega\$.

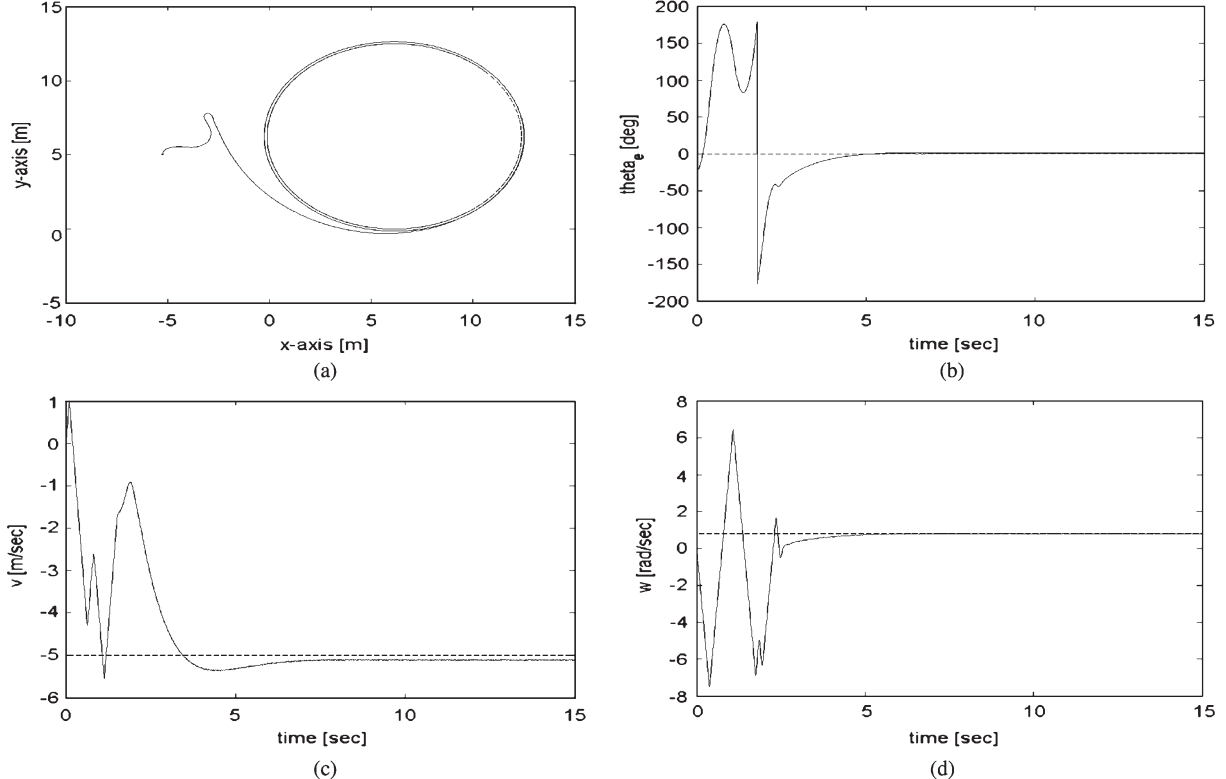


Fig. 5. Trajectory tracking performance of the proposed controller with input saturation (31) (Scenario 3). In (a), (c), and (d), (dashed) reference and (solid) proposed. (a) \$x\$-\$y\$ plot. (b) Tracking error (\$\theta_e\$). (c) Forward velocity \$v\$. (d) Angular velocity \$\omega\$.

In Scenario 5, only the result of the proposed controller is shown in Figs. 5(a), 7(a), and 8(a), as the controller in [18] is proposed for tracking a reference moving only in the forward direction.

Fig. 3(a) shows that a straight line can be exactly followed by the proposed method with the convergence of the position tracking errors to zero, whereas the previous controller in [18] showed a degraded transient performance. Fig. 3(b) shows that

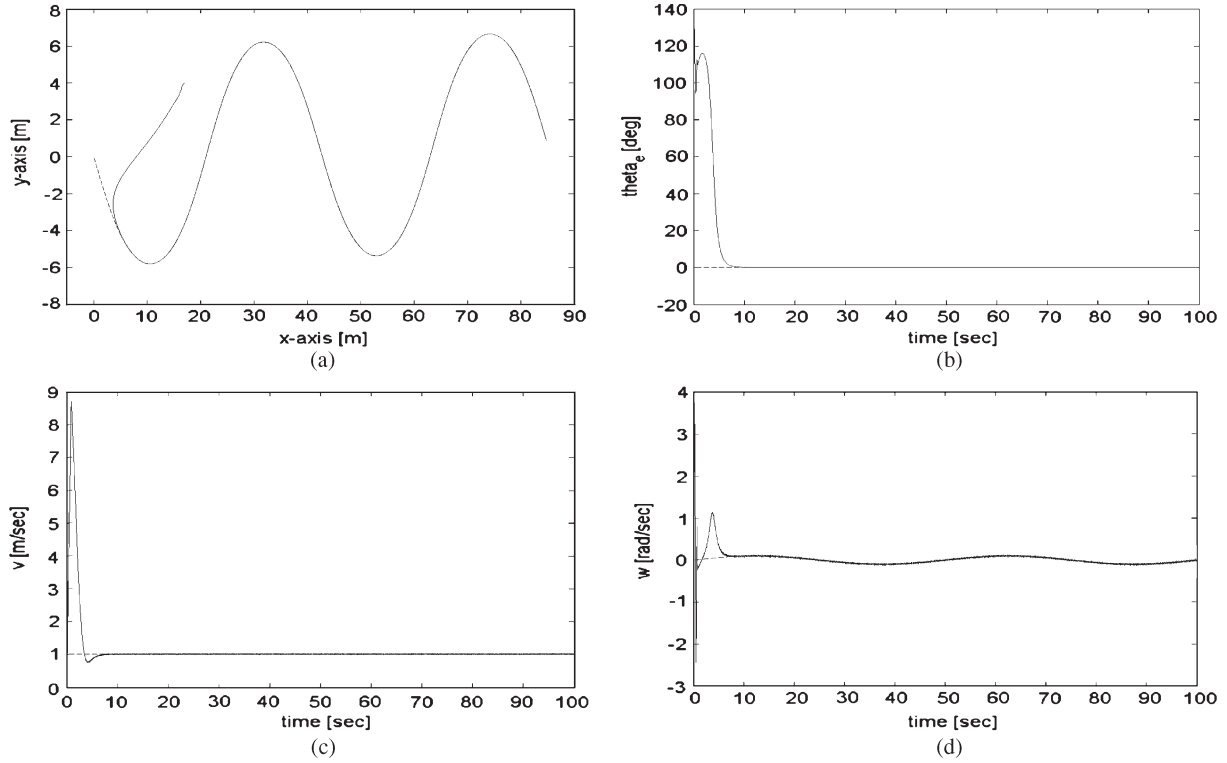


Fig. 6. Trajectory tracking performance of the proposed controller with input saturation (31) (Scenario 4). In (a), (c), and (d), (dashed) reference and (solid) proposed. (a) x - y plot. (b) Tracking error (θ_e). (c) Forward velocity v . (d) Angular velocity ω .

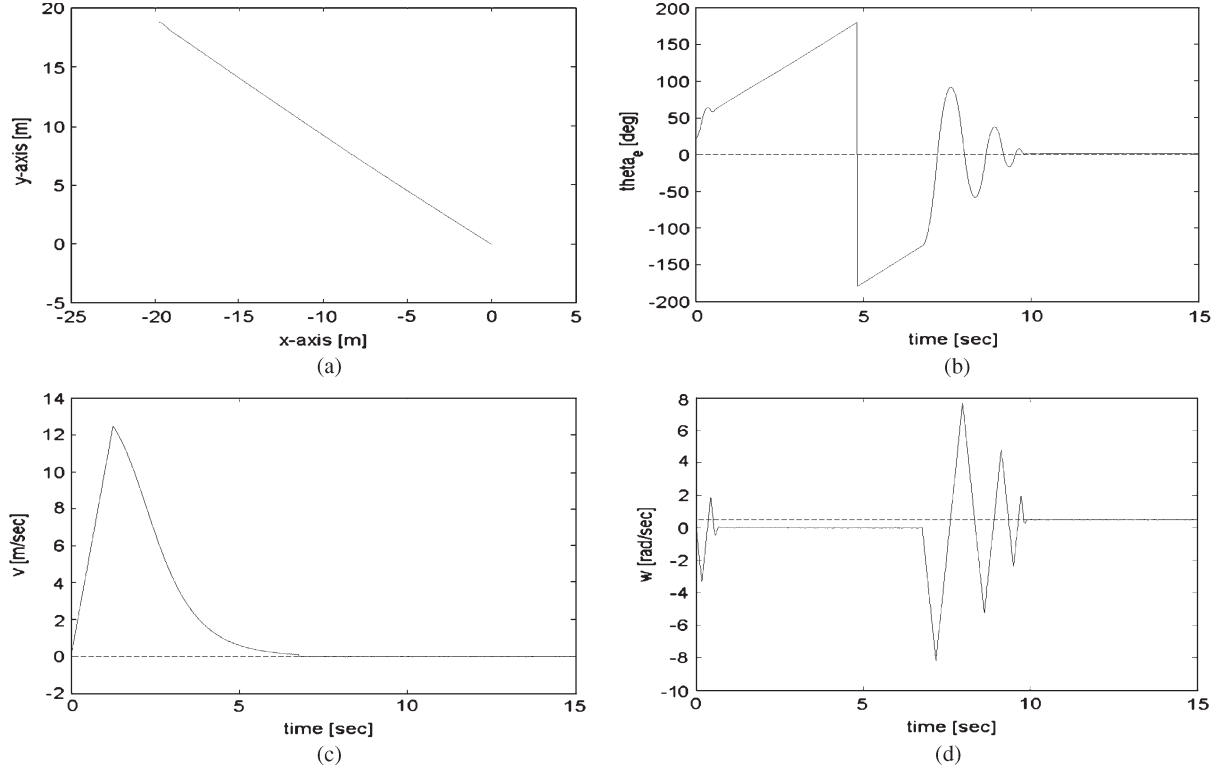


Fig. 7. Trajectory tracking performance of the proposed controller with input saturation (31) (Scenario 5). In (a), (c), and (d), (dashed) reference and (solid) proposed. (a) x - y plot. (b) Tracking error (θ_e). (c) Forward velocity v . (d) Angular velocity ω .

the tracking error of the heading direction angle converges to zero. Fig. 3(c) and (d) shows that the actual velocities converge to the reference velocities. Figs. 4 and 5 show that the tracking

performance of the proposed controller is satisfactory, when the reference angular velocity is negative, as in the case of Scenario 2, or even when the reference forward velocity is

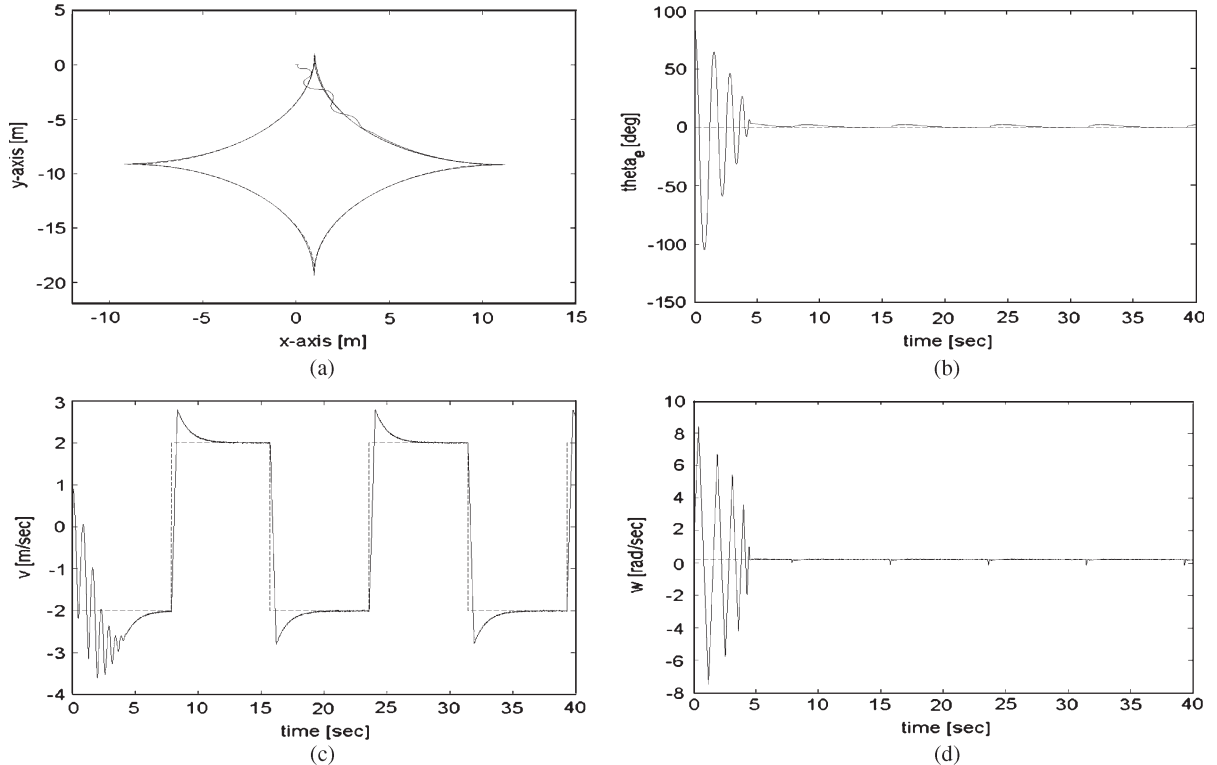


Fig. 8. Trajectory tracking performance of the proposed controller with input saturation (31) (Scenario 6). In (a), (c), and (d), (dashed) reference and (solid) proposed. (a) x - y plot. (b) Tracking error (θ_e). (c) Forward velocity v . (d) Angular velocity ω .

negative, as in the case of Scenario 3. Fig. 6 shows that a sinusoidal trajectory can be followed as the tracking errors become near zero and also shows better results than the method described in [12]. We did not include the performance of the previous method [18] in Fig. 6(a), since a previous controller in [18] showed a highly degraded performance in the case of Scenario 4 due to the input saturation [see (31)]. Fig. 7 shows that the reference spinning trajectory with no forward velocity and a nonzero rotational velocity in Scenario 5 can be followed. Finally, the reference trajectory in Scenario 8, which changes the sign of the forward velocity as the quadrant of the heading direction angle changes, can be followed, as shown in Fig. 8. In particular, the forward velocity can be followed satisfactorily, as shown in Fig. 8(c). These results demonstrate that the proposed method results in a satisfactory tracking performance even in the presence of dynamic disturbances and input saturation in both velocities and accelerations.

V. CONCLUSION

In this paper, a tracking control method for differential-drive wheeled mobile robots has been proposed using backstepping-like feedback linearization. A global ultimate boundedness of tracking errors is obtained, and the corresponding ultimate bound can be adjusted by control parameters. These features are also demonstrated in numerical simulations, where various reference trajectories, including a straight line, a circle, a sinusoidal curve, a spinning trajectory with no forward linear velocity and a nonzero rotational velocity, a cross-shaped trajectory with the changing of the forward and backward directions,

etc., are followed with sufficiently small position and heading direction angle tracking errors.

As the proposed modular control structure can make the separate design of kinematic and dynamic controllers possible, the proposed kinematic controller and a (model-free) PID dynamic controller can be simply combined, in which case, however, the overall tracking performance may not be sufficient due to the limited dynamic compensation. Thus, an additional scheme for the compensation of the dynamic properties should be developed to have a better tracking control performance. Considering the fact that the exact information on dynamics is difficult to know, further work on dynamic control (based on a neural network, fuzzy control, etc.) can be pursued as a future work.

REFERENCES

- [1] I. Kolmanovsky and N. H. McClamroch, "Developments in nonholonomic control problems," *IEEE Control Syst. Mag.*, vol. 15, no. 6, pp. 20–36, Dec. 1995.
- [2] F. Zhang, Y. Xi, Z. Lin, and W. Chen, "Constrained motion model of mobile robots and its applications," *IEEE Trans. Syst., Man, Cybern. B, Cybern.*, vol. 39, no. 3, pp. 773–787, Jun. 2009.
- [3] C.-H. Lin and C.-T. King, "Sensor-deployment strategies for indoor robot navigation," *IEEE Trans. Syst., Man, Cybern. A, Syst., Humans*, vol. 40, no. 2, pp. 388–398, Mar. 2010.
- [4] C. Giovannangeli and P. Gaussier, "Interactive teaching for vision-based mobile robots: A sensory-motor approach," *IEEE Trans. Syst., Man, Cybern. A, Syst., Humans*, vol. 40, no. 1, pp. 13–28, Jan. 2010.
- [5] T. Dierks and S. Jagannathan, "Neural network control of mobile robot formations using RISE feedback," *IEEE Trans. Syst., Man, Cybern. B, Cybern.*, vol. 39, no. 2, pp. 332–347, Apr. 2009.
- [6] M. Bugeja, S. G. Fabri, and L. Camilleri, "Dual adaptive dynamic control of mobile robots using neural networks," *IEEE Trans. Syst., Man, Cybern. B, Cybern.*, vol. 39, no. 1, pp. 129–141, Feb. 2009.

- [7] N. Bellotto and H. Hu, "Multisensor-based human detection and tracking for mobile service robots," *IEEE Trans. Syst., Man, Cybern. B, Cybern.*, vol. 39, no. 1, pp. 167–181, Feb. 2009.
- [8] R. W. Brockett, "Asymptotic stability and feedback linearization," in *Differential Geometric Control Theory*, R. W. Brockett, R. S. Millman, and H. J. Sussman, Eds. Boston, MA: Birkhauser, 1983, pp. 181–191.
- [9] Z.-P. Jiang and H. Nijmeijer, "Tracking control of mobile robots: A case study in backstepping," *Automatica*, vol. 33, no. 7, pp. 1393–1399, Jul. 1997.
- [10] Z.-P. Jiang, E. Lefeber, and H. Nijmeijer, "Saturated stabilization and tracking of a nonholonomic mobile robot," *Syst. Control Lett.*, vol. 42, no. 5, pp. 327–332, Apr. 2001.
- [11] T.-C. Lee, K.-T. Song, C.-H. Lee, and C.-C. Teng, "Tracking control of unicycle-modeled mobile robots using a saturation feedback controller," *IEEE Trans. Control Syst. Technol.*, vol. 9, no. 2, pp. 305–318, Mar. 2001.
- [12] P. Encarnação and A. Pascoal, "Combined trajectory tracking and path following control for dynamic wheeled mobile robots," in *Proc. 15th IFAC World Congr. Autom. Control*, Barcelona, Spain, Jul. 2002.
- [13] M. Aicardi, G. Casalino, A. Bicchi, and A. Balestrino, "Closed loop steering of unicycle like vehicles via Lyapunov techniques," *IEEE Robot. Autom. Mag.*, vol. 2, no. 1, pp. 27–35, Mar. 1995.
- [14] G. Indiveri, "Kinematic time-invariant control of a 2D nonholonomic vehicle," in *Proc. 38th Conf. Decision Control*, Phoenix, AZ, Dec. 1999, pp. 2112–2117.
- [15] Y.-C. Chang and B.-S. Chen, "Adaptive tracking control design of nonholonomic mechanical systems," in *Proc. Conf. Decision Control*, Kobe, Japan, Dec. 1996, pp. 4739–4744.
- [16] T. Fukao, H. Nakagawa, and N. Adachi, "Adaptive tracking control of a nonholonomic mobile robot," *IEEE Trans. Robot. Autom.*, vol. 16, no. 5, pp. 609–615, Oct. 2000.
- [17] D. Chwa, "Sliding mode tracking control of nonholonomic wheeled mobile robots in polar coordinates," *IEEE Trans. Control Syst. Technol.*, vol. 12, no. 4, pp. 637–644, Jul. 2004.
- [18] Y. Kanayama, Y. Kimura, F. Miyazaki, and T. Noguchi, "A stable tracking control method for an autonomous mobile robot," in *Proc. IEEE Int. Conf. Robot. Autom.*, Cincinnati, OH, 1990, pp. 384–389.
- [19] C. Canudas de Wit and O. J. Sordalen, "Exponential stabilization of mobile robot with nonholonomic constraints," *IEEE Trans. Autom. Control*, vol. 37, no. 11, pp. 1791–1797, Nov. 1992.
- [20] B. d'Andréa-Novel, G. Campion, and G. Bastin, "Control of nonholonomic wheeled mobile robots by state feedback linearization," *Int. J. Robot. Res.*, vol. 14, no. 6, pp. 543–559, Dec. 1995.
- [21] T.-H. S. Li and S.-J. Chang, "Autonomous fuzzy parking control of a car-like mobile robot," *IEEE Trans. Syst., Man, Cybern. A, Syst., Humans*, vol. 33, no. 4, pp. 451–465, Jul. 2003.
- [22] H. C.-H. Hsu and A. Liu, "A flexible architecture for navigation control of a mobile robot," *IEEE Trans. Syst., Man, Cybern. A, Syst., Humans*, vol. 37, no. 3, pp. 310–318, May 2007.
- [23] J. L. Crowley, "Asynchronous control of orientation and displacement in a robot vehicle," in *Proc. IEEE Conf. Robot. Autom.*, Scottsdale, AZ, May 14–19, 1989, pp. 1277–1282.
- [24] O. Amidi, "Integrated mobile robot control," *Robot. Inst.*, Carnegie Mellon Univ., Pittsburgh, PA, Tech. Rep. CMU-RI-TR-90-17, May 1990.
- [25] C.-Y. Su and Y. Stepanenko, "Robust motion/force control of mechanical systems with classical nonholonomic constraints," *IEEE Trans. Autom. Control*, vol. 39, no. 3, pp. 609–614, Mar. 1994.
- [26] C. F. Lin, *Modern Navigation, Guidance, and Control Processing*. Englewood Cliffs, NJ: Prentice-Hall, 1992.
- [27] M. Saeki and Y. Sakae, "Flight control design for a nonlinear non-minimum phase VTOL aircraft via two-step linearization," in *Proc. 40th IEEE Conf. Decision Control*, Orlando, FL, Dec. 2001, pp. 217–222.
- [28] R. Sepulchre, M. Jankovic, and P. Kokotovic, *Constructive Nonlinear Control*. Berlin, Germany: Springer-Verlag, 1997.
- [29] H. K. Khalil, *Nonlinear Systems*, 3rd ed. Englewood Cliffs, NJ: Prentice-Hall, 1996.



Dongkyoung Chwa received the B.S. and M.S. degrees from Seoul National University, Seoul, Korea, in 1995 and 1997, respectively, and the Ph.D. degree from the School of Electrical and Computer Engineering, Seoul National University, in 2001.

From 2001 to 2003, he was a Postdoctoral Researcher with Seoul National University, where he was a BK21 Assistant Professor in 2004. In 2003, he was a Visiting Research Fellow with the University of New South Wales, Australian Defence Force Academy, Canberra, Australia, and the Honorary

Visiting Academic with the University of Melbourne, Melbourne, Australia. Since 2005, he has been with the Department of Electrical and Computer Engineering, Ajou University, Suwon, Korea, where he is currently an Associate Professor. His research interests are nonlinear, robust, and adaptive control theories and their applications to robotics, underactuated systems including wheeled mobile robots, underactuated ships, cranes, and guidance and control of flight systems.